Elsevier Editorial System(tm) for Advances in Space Research
Manuscript Draft

Manuscript Number: ASR-D-14-00203R1

Title: Automatic interpretation of oblique ionograms

Article Type: EM -Earth Magnetosphere/Upper Atmosphere

Keywords: Ionosphere; Electron density; Oblique ionograms; MUF.

Corresponding Author: Dr. Alessandro Settimi, Ph.D

Corresponding Author's Institution: Istituto Nazionale di Geofisica e Vulcanologia (INGV)

First Author: Alessandro Ippolito, Dr.

Order of Authors: Alessandro Ippolito, Dr.; Carlo Scotto, Senior Researcher; Matthew Francis, Dr.; Alessandro Settimi, Ph.D; Claudio Cesaroni, Dr.

Abstract: We present an algorithm for the identification of trace characteristics of oblique ionograms allowing determination of the Maximum Usable Frequency (MUF) for communication between the transmitter and receiver. The algorithm automatically detects and rejects poor quality ionograms. We performed an exploratory test of the algorithm using data from a campaign of oblique soundings between Rome, Italy (41.90 N, 12.48 E) and Chania, Greece (35.51 N, 24.01 E) and also between Kalkarindji, Australia (17.43 S, 130.81 E) and Culgoora, Australia (30.30 S, 149.55 E). The success of these tests demonstrates the applicability of the method to ionograms recorded by different ionosondes in various helio and geophysical conditions.

Response to Reviewers:

Cover letter to Editor

Dear Adv. Space Res. Editor in Chief, Jan Laštovicka,
this cover letter is for re-submitting our manuscript (ASR-D-14-00203), entitled as:

“Automatic interpretation of oblique ionograms",

by the Authors,

Alessandro Ippolito, Carlo Scotto, Matthew Francis, Alessandro Settimi, Claudio Cesaroni.

We would like thanking the Reviewers 1 and 2 for their useful suggestions. We agree with them. We tried to change the paper in all the points that the Reviewers have suggested. We have provided detailed explanations in the attached reply letters.

We would like adjoining Dr. Matthew Francis as Co-author, acknowledging his substantial suggestions to improve our article.

Please, let me know of your decision at your earliest convenience.

With my best regards,
Sincerely yours,
Alessandro Settimi, PhD.

Reply to Reviewer 1

Click here to download Detailed Response to Reviewers: Reply to Reviewer 1.docx

"Automatic interpretation of oblique ionograms"

Manuscript Number: ASR-D-14-00203

Section: Earth magnetosphere and Upper Atmosphere Article

Title: Automatic interpretation of oblique ionograms Advances in Space Research

Editor:

In fact the revision is medium revision on half way between minor and major revision.

Reviewers' comments:

Please note that editors and/or reviewers have uploaded files related to this submission. To access these file(s) while you are not logged into the system, please click on the link below. (Note: this link will expire after 5 clicks or 30 days.) Alternatively, you may log in to the system and click the 'View Review Attachments' link in the Action column.

http://ees.elsevier.com/asr/l.asp?i=64119&l=AGSI7ZRU

Authors:

The minor corrections have been accepted and introduced in the manuscript.

Concerning the most relevant issues:

1) Pag. 7

We wrote: "In this way, for each pair of curves, the local correlation $C(f_{v\_ord}, \delta_{f\_ord}, t_{v\_ord}, \delta_{t\_ord}, f_{v\_ext}, \delta_{f\_ext}, t_{v\_ext}, \delta_{t\_ext})$ with the ionogram recorded is calculated, and the pair of curves s_{ord} and s_{ext} with the maximum C value, called C_{max}, is selected".

Your comment was: "It is worthy to explain the calculation of correlation parameter C".

We rewrote: "C is the value of the contrast between the pair of empirical curves used to represent the ordinary and extraordinary traces, calculated with the same techniques used in the electronic processing of the images".

2) Pag. 9

We wrote: "threshold C_t".

Your comment was: "How the threshold is posed?".

We rewrote: "In Tabs. 2 we describe the accuracy of the automatic scaling for using different C_t. It can be clearly seen how the best results are obtained for $C_t = 225$ (Tab. 1(d)), as it allows to have the best result in terms of percentage of accurate autoscaled ionograms versus false positive event".

3) Pag. 9

We wrote: "The most critical cases are the ionograms not discarded by the software, but for which an operator was unable to provide the MUF value".

Your comment was: “It would be good to add some figures to present such a case as an example, as well as for the cases that the program performs worse and the same as or better than the experienced operator”.

We put an example as you suggested and we rewrote: “In Fig. 3 we show an example of the most critical cases, for which the ionograms are not discarded by the software, but an operator was unable to provide the MUF value”.

4) Section 4

Your comment was: “It is my opinion that section 4 should be either removed (leaving a paper of very limited scope but some value) or the work of this section should be expanded and completed to the point where results can be demonstrated”.

We have removed section 4 from this work as we added new results from the autoscaling algorithm. We will expand and complete the description of our eikonal based ray tracing in a future manuscript.

"Automatic interpretation of oblique ionograms"

Manuscript Number: ASR-D-14-00203

Section: Earth magnetosphere and Upper Atmosphere Article

Title: Automatic interpretation of oblique ionograms Advances in Space Research

Editor:

In fact the revision is medium revision on half way between minor and major revision.

Reviewer #2:

This paper describes an algorithm for the automatic detection of oblique ionogram MUF created by adapting the autoscala algorithm normally applied to VIS ionograms.

This paper also describes partial and preliminary results of inverting this scaled data into a midpoint electron density profile assuming a spherically symmetric ionosphere.

The material is new and interesting and the subject of this paper (automatic scaling of oblique ionograms for ionospheric monitoring and inclusion in models) is important.

The language is clear and well written and the referencing is adequate.

My major concern with this paper is too much of the content is incomplete to meet the standard of Advances in Space Research.

On this basis I recommend the article be reconsidered after revision.

Elements of this revision that the authors might consider are;

In section 3 the results of testing the algorithm are tabulated in table 1 and table 2. While the tabulation of results is valuable, the nature of the results might be better understood by presenting a time series plot of raw data and estimated MUF e.g. a time series of results over-plotted on an historical band availability (HBA) plot. This would make clearer to the reader the environmental

diversity captured in the sample of 264 ionograms under test and hence how the paper's algorithms might be expected to perform under a wider range of conditions.

Also the algorithm would be more clearly understood by the reader if there was some discussion or presentation of the achieved strength of correlation and the examples of the impact of different Cmax and the impact of different delta_ford etc controlling the size of the region within the correlation assessment. …

Authors: We tested the algorithm on the same ionogram data set, using three different contrast threshold values and for different geomagnetic K_p indices. In Tabs. 1 and 2 we report a comparison between the numbers of the ionograms scaled by the operator and the ones automatically scaled by our program. It can be seen that for higher values of contrast threshold, the number of false positive events decreases.

We show, in the time series plots on Fig. 2, the difference between the autoscaled MUFs and the manual scaled ones. The colours represent the different values of K_p index associated to each autoscaled ionogram, in order to describe different geomagnetic conditions.

The program performances are not influenced by changing K_p values: as one can see from Fig. 2, the number of autoscaled ionograms only depends on the contrast threshold value. This demonstrates a good behaviour of our autoscaling algorithm under different geomagnetic conditions.

Reviewer #2: … In section 4, the authors sketch a methodology to invert the extracted trace information into a midpoint electron density profile assuming a spherically symmetric ionosphere. At different points in the paper the authors speak of the ionosphere being represented by a single variable layer (described by three parameters or points) or the more normal day time conditions when there are several layers present simultaneously. There is no explanation in the paper concerning how this algorithm can be used to prescribe a complete electron density profile when so much of the trace extracted from the image is potentially incomplete.

It is my opinion that section 4 should be either removed (leaving a paper of very limited scope but some value) or the work of this section should be expanded and completed to the point where results can be demonstrated.

Authors: As suggested we have decided to remove section 4 from this work as we added new results from the autoscaling algorithm. We will expand and complete the description of our eikonal based ray tracing in a future manuscript.

Highlights

An algorithm for identifying the trace characteristics of oblique ionograms.

Determining the MUF in relation to the distance between TX and RX.

Some results of an exploratory test.

Automatic interpretation of oblique ionograms

Alessandro Ippolito[(1,3)], *Carlo Scotto*[(1)], *Matthew Francis*[(2)],

Alessandro Settimi[(1)*], *Claudio Cesaroni*[(1,3)]

[(1)] Istituto Nazionale di Geofisica e Vulcanologia (INGV),

Sezione di Geomagnetismo, Aeronomia e Geofisica Ambientale (ROMA 2),

Via di Vigna Murata 605, I-00143 Rome, Italy

[(2)] IPS Radio & Space Services,

Bureau of Meteorology,

Level 15, Tower C, 300 Elizabeth Street, Sydney, Australia

[(3)]Doctoral School of Geophysics,

ALMA MATER STUDIORUM, Università di Bologna,

Via Zamboni 33, I-40126 Bologna, Italy

*Corresponding author: Alessandro Settimi; Tel: +39-06-51860719; Fax: +39-06-51860397; Email: alessandro.settimi@ingv.it;

Co-authors email addresses: Alessandro Ippolito: alessandro.ippolito@ingv.it; Carlo Scotto: carlo.scotto@ingv.it; Matthew Francis: M.Francis@bom.gov.au; Claudio Cesaroni: claudio.cesaroni@ingv.it

Abstract

We present an algorithm for the identification of trace characteristics of oblique ionograms allowing determination of the Maximum Usable Frequency (MUF) for communication between the transmitter and receiver. The algorithm automatically detects and rejects poor quality ionograms. We performed an exploratory test of the algorithm using data from a campaign of oblique soundings between Rome, Italy (41.90 N, 12.48 E) and Chania, Greece (35.51 N, 24.01 E) and also between Kalkarindji, Australia (17.43 S, 130.81 E) and Culgoora, Australia (30.30 S, 149.55 E). The success of these tests demonstrates the applicability of the method to ionograms recorded by different ionosondes in various helio and geophysical conditions.

Keywords: Ionosphere; Electron density; Oblique ionograms; MUF.

1. Introduction

The variable state of the ionosphere is generally monitored by networks of vertical ionosondes, providing real-time information on the state of the ionosphere. An oblique ionospheric sounder extends this concept: the transmitter and receiver of an oblique sounder are not co-located, unlike vertical sounders, and are generally several hundreds or thousands of kilometers apart, so that the instrumentation is able to study how High Frequency (HF) radio signals propagate via the ionosphere under a variety of conditions.

For vertical ionograms there are well-established techniques that make it possible to obtain the main physical parameters of the ionosphere in real-time. These include the ARTIST system (Reinisch and Huang, 1983; Gilbert and Smith, 1988; Galkin et al. 2008) developed at the University of Lowell,

Center for Atmospheric Research, and the Autoscala program from the Italian "Istituto Nazionale di Geofisica e Vulcanologia (INGV)" (Scotto and Pezzopane, 2002; Pezzopane and Scotto, 2007; Scotto 2009). The data produced by these computer programs can be effectively integrated in real-time and short term forecasting models (Galkin et al. 2012). However, the interpretation of oblique ionograms is significantly more complex, and there are no well established automatic techniques.

The reason for the lack of such techniques is partly due to the relatively rare use of this type of sounding, at least in a systematic way, with the consequence of less effort being dedicated to them. Undoubtedly, it is also due to the greater difficulties that these ionograms pose compared to vertical soundings. On the other hand, the information obtained from an oblique HF sounder is much more articulated than that derived from traditional vertical ionogram readings. Noteworthy in this respect are the attempts of Huang et al. (1996) to develop a computationally efficient technique for the inversion of oblique inograms, in order to obtain mid-point electron density profiles.

The reason that the inversion of an oblique ionogram is much more difficult than the inversion of a vertical one is because an obliquely propagating radio wave is refracted and not just reflected, making it far more prone to the effects of horizontal gradients and variations in the ionosphere, and posing significant problems for ray-tracing (Norman and Cannon, 1999). The situation is further complicated by the fact that radio signals from a transmitter can take a variety of different paths to reach the receiver, adding possible sources of signal distortion and loss.

Oblique ionograms provide high-resolution images that permit quick identification of the frequencies that are propagating between given transmitter and receiver stations. They also reveal the available communication bands and the gaps where no links can be established. These characteristics of a channel are very important because the information on available frequencies needs constant update, considering that the ionosphere changes on a time scale of every few minutes.

In the absence, until now, of software for automatic interpretation, oblique soundings have largely been used to try to understand the factors aggravating propagation in order to reduce radio link unreliability produced by natural ionospheric variability. Oblique ionospheric sounding also offer several important advantages over vertical sounding for the understanding of radio wave propagation. For example the possibility to monitor the ionosphere across large otherwise inaccessible distances, like the oceans.

The greater complexity of oblique compared to vertical ionograms is matched by greater informational content, affording to this technique enormous potential, which, in the opinion of the authors, has not yet been fully exploited. It is perfectly reasonable to presume that ionospheric structure can be determined from an oblique ionogram, albeit with much greater difficulty than from a vertical ionogram.

2. An algorithm for the automatic scaling of oblique ionograms

The software developed in this study, initially stores an ionogram as a matrix *A*, with *m* rows and *n* columns, as defined by the following formulas:

$$m = \mathrm{int}\left[\frac{t_f - t_0}{\Delta_f}\right] + 1 \tag{1}$$

and

$$n = \mathrm{int}\left[\frac{f_f - f_0}{\Delta_f}\right] + 1 \tag{2}$$

where f_f, f_0, Δ_f, t_f, t_0, Δ_t, are respectively the final frequency, the initial frequency, the frequency step, the final time delay, the initial time delay, and the time delay resolution of the oblique sounding. In general, t_0, Δ_t are fixed values, which depend on the design of the ionosonde. The transmitting system is based on a VOS-1 chirp ionosonde produced by the Barry Research Corporation, Palo Alto, CA, USA [Barry Research Corporation, 1975] sweeping from 2 to 30 MHz at 100 kHz/s with an average power of less than 10 W. The transmitting antenna is a delta for decametric wavelength used for vertical soundings, suited for oblique soundings. The receiver is an RCS-5B chirp produced by the Barry Research Corporation [1989]. The element a_{ij} (with i = 1, ..., m and j = 1, ..., n) of the matrix A is an integer ranging from 0 to 255 proportional to the amplitude of received echo, this value being obtained directly from the binary file recorded by the instrument.

Once the ionogram is stored in the form of a matrix of elements a_{ij}, two empirical curves s_{ord} and s_{ext} are defined, each of which is the branch of a parabola. These two curves are able to fit the typical shapes of the ordinary and extraordinary oblique ionogram traces resulting from a single reflection in the F2 region. The curve s_{ord}, which is used for the investigation of the ordinary trace, is:

$$t_{ord}=\text{int}[A_{ord}\cdot f^2+B_{ord}\cdot f+C_{ord}], \tag{3}$$

where f varies within the limits:

$$f_{v\_ord}-\delta_{f\_ord} \le f \le f_{v\_ord}. \tag{4}$$

The coefficients A_{ord}, B_{ord}, and C_{ord} are related to f_{v_ord}, δ_{f_ord}, t_{v_ord}, δ_{t_ord} by the following relationships:

$$A_{\text{ord}} = -\frac{(\delta_{\text{f\_ord}} - f_{\text{v\_ord}})}{\delta_{\text{t\_ord}}^{\,2}} - \frac{f_{\text{v\_ord}}}{\delta_{\text{t\_ord}}^{\,2}}, \tag{5}$$

$$B_{ord} = \frac{2(\delta_{\text{f\_ord}} - f_{\text{v\_ord}}) \cdot t_{\text{v\_ord}}}{\delta_{\text{t\_ord}}^{\,2}} + \frac{2 \cdot f_{\text{v\_ord}} \cdot t_{\text{v\_ord}}}{\delta_{\text{t\_ord}}^{\,2}}, \tag{6}$$

and

$$C_{\text{ord}} = -\frac{(\delta_{\text{f\_ord}} - f_{\text{v\_ord}}) \cdot t_{\text{v\_ord}}^{\,2}}{\delta_{\text{t\_ord}}^{\,2}} + \frac{f_{v\_ord} \cdot (\delta_{\text{t\_ord}}^{\,2} - t_{\text{v\_ord}}^{\,2})}{\delta_{\text{t\_ord}}^{\,2}}. \tag{7}$$

Similarly, for the curve s_{ext}, used for the investigation of the extraordinary ray:

$$t_{\text{ext}} = \text{int}[A_{\text{ext}} \cdot f^{\,2} + B_{\text{ext}} \cdot f + C_{\text{ext}}], \tag{8}$$

where f varies within the limits:

$$f_{\text{v\_ext}} - \delta_{\text{f\_ext}} \le f \le f_{\text{v\_ext}}. \tag{9}$$

The coefficients A_{ext}, B_{ext}, and C_{ext} are related to $f_{\text{v\_ext}}$, $\delta_{\text{f\_ext}}$, $t_{\text{v\_ext}}$, $\delta_{\text{t\_ext}}$ by the following relationships:

$$A_{\text{ext}} = -\frac{(\delta_{\text{f\_ext}} - f_{\text{v\_ext}})}{\delta_{\text{t\_ext}}^{\,2}} - \frac{f_{\text{v\_ext}}}{\delta_{\text{t\_ext}}^{\,2}}, \tag{10}$$

$$B_{\text{ext}} = \frac{2(\delta_{\text{f\_ext}} - f_{\text{v\_ext}}) \cdot t_{\text{v\_ext}}}{\delta_{\text{t\_ext}}^{\,2}} + \frac{2 \cdot f_{\text{v\_ext}} \cdot t_{\text{v\_ext}}}{\delta_{\text{t\_ext}}^{\,2}}, \tag{11}$$

and

$$C_{\text{ext}} = -\frac{(\delta_{\text{f\_ext}} - f_{\text{v\_ext}}) \cdot t_{\text{v\_ext}}^{\,2}}{\delta_{\text{t\_ext}}^{\,2}} + \frac{f_{\text{ext}} \cdot (\delta_{\text{t\_ext}}^{\,2} - t_{\text{v\_ext}}^{\,2})}{\delta_{\text{t\_ext}}^{\,2}}. \tag{12}$$

The frequencies and time delays of s_{ord} and s_{xt} are expressed as integers and correspond to the indices i and j of the matrix *A*. The parameters defining the two curves are:

$$f_{\text{v\_ord}}, \delta_{\text{f\_ord}}, t_{\text{v\_ord}}, \delta_{\text{t\_ord}}, f_{\text{v\_ext}}, \delta_{\text{f\_ext}}, t_{\text{v\_ext}}, \delta_{\text{t\_ext}}\ .$$

Two integers $f_{\text{v\_ord}}$, and $t_{\text{v\_ord}}$, are the vertex coordinates in pixels of s_{ord}. Two integers $\delta_{\text{t\_ord}}$ and $\delta_{\text{t\_ext}}$ vary from 3 to 60 and correspond to the width values for both s_{ord} and s_{ext} expressed in pixels, along the *t* axis; the integers $\delta_{\text{f\_ord}}$ and $\delta_{\text{f\_ext}}$, fixed at 30, represent the extensions in pixels along the *f* axis of the two branches of the parabola. The abscissa vertex coordinates in pixels of s_{ext}, $f_{\text{v\_ext}}$, is linked with $f_{\text{v\_ord}}$ through the relation $f_{\text{v\_ext}} = f_{\text{v\_ord}} + \Delta f_{\text{ord-ext}}$. $\Delta f_{\text{ord-ext}}$ corresponds to a frequency of about 0.6 MHz, expressed in pixels. The ordinate vertex coordinates in pixels of s_{ext} varies from $t_{\text{v\_ord}}$ to ($t_{\text{v\_ord}}$ + 20). The s_{ord} curve (and consequently s_{ext}) is slid across the entire ionogram, and so $f_{\text{v\_ord}}$ varies from $\delta_{\text{f\_ord}}$ to n - $\Delta f_{\text{ord-ext}}$, while $t_{\text{v\_ord}}$ varies from $\delta_{\text{t\_ord}}$ to *m*. Furthermore, varying the parameters, and thus causing s_{ord} and s_{ext} to change shape, while maintaining consistency with the typical oblique ionogram trace shape, results in the vertices moving throughout the ionogram. In this way, for each pair of curves, the local correlation $C(f_{\text{v\_ord}}, \delta_{\text{f\_ord}}, t_{\text{v\_ord}}, \delta_{\text{t\_ord}}, f_{\text{v\_ext}}, \delta_{\text{f\_ext}}, t_{\text{v\_ext}}, \delta_{\text{t\_ext}})$ with the ionogram recorded is calculated. In practice, *C* is the value of the contrast between

the pair of empirical curves used to represent the ordinary and extraordinary traces, calculated with the same techniques used in the electronic processing of the images. The pair of curves s_{ord} and s_{ext} with the maximum C value, called C_{max}, is then selected as shown in Fig. 1. The Maximum Usable Frequency (MUF) resulting from the specified oblique sounding can then be inferred from the point V_{ord} of coordinates (f_{v_ord}; t_{v_ord}).This method also provides a criterion for discarding ionograms that do not have sufficient information. Only if C_{max} is larger than a fixed threshold C_t, the resulting curves, are considered representative of the trace due to reflection from the F2 region. Otherwise, the ionogram is considered to lack sufficient information and is discarded. In this case, no MUF value is provided as output.

3. Behaviour of the algorithm

The problem of assessing the behaviour of scaling algorithms has been successfully resolved for vertical inograms by various authors (Scotto and Pezzopane, 2002; Scotto and Pezzopane, 2004; Stankov et al., 2012, Cesaroni et al., 2013). In order to evaluate the errors in the data generated by the programs' automatic operation, all these authors made the obvious decision of comparing the program results with the data produced manually by an experienced operator.

Following this approach 272 oblique ionograms were automatically scaled and classified into two groups: subset Y containing ionograms successfully scaled by the software, and subset N containing ionograms considered by the software to lack sufficient information, according to the criterion discussed above.

For each of these subsets was then considered:

a) The number of ionograms for which an operator was able to determine the MUF;

b) The number of ionograms for which an operator was unable to determine the MUF.

Furthermore, a quantitative comparison was performed between the manually scaled values and the corresponding automatically scaled values. Naturally, this analysis was limited to the cases in which both the operator and the software were able to scale the ionogram. In this study, a value generated by the software was considered accurate if it lies within 0.5 MHz from the one provided by the operator, while a value was acceptable if it lies within 2.5 MHz. These limits were chosen in line with the International Union of Radio Science (URSI) standard (Piggott and Rawer, 1972).

These procedures have been applied to a data set of 272 ionograms, using five different C_t. In this way, it is also possible to evaluate the appropriate C_t value to be fixed. In Tabs. 1 we report a comparison between the numbers of the ionograms scaled by the operator and the ones automatically scaled by our program. It can be seen that for higher values of C_t, the number of false positive events decreases. In Tabs. 2 we describe the accuracy of the automatic scaling for using different C_t. It can be clearly seen how the best results are obtained for $C_t = 225$ (Tab. 1(d)), as it allows to have the best result in terms of percentage of accurate autoscaled ionograms versus false positive event.

We show, in the time series plots on Fig. 2, the difference between the autoscaled MUFs and the manual scaled ones, for three values of C_t. The colours represent the different values of K_p index associated to each autoscaled ionogram, in order to describe different geomagnetic conditions. As one can see the program performances are not influenced by changing K_p values and the number of autoscaled ionograms only depends on C_t. This demonstrates a good behaviour of our autoscaling algorithm under different geomagnetic conditions.

In Fig. 3 we show an example of the most critical cases, for which the ionograms are not discarded by the software, but an operator was unable to provide the MUF value. Furthermore, it is important to note that the algorithm does not discard ionograms that have a well defined trace, from point of view of an operator.

In any case, the presence in the database of a high percentage of low quality ionograms, makes it possible to efficiently assess the rejection capabilities of the program. The rejection of low quality ionograms is, in fact, a major problem in Space Weather applications. It has been demonstrated that the integration of erroneous data into models has negative effects on the reliability of now-casting and short-term forecasting models, and it is considered preferable to discard questionable data (Galkin, 2012).

It has been possible to study the behaviour of the software more rigorously exploiting the wide IPS ionogram database. Following the same procedure described before, we used a restricted data base of 202 ionograms from oblique radio soundings campaigns performed on the path of 2380 km between Kalkarindji, (17.43 S, 130.81 E) and Culgoora, Australia (30.30 S, 149.55 E) to perform numerical experiments. The IPS oblique ionograms were recorded using a Digital Oblique Receiving System (DORS) on loan from the Australian Defence Science and Technology Organisation (DSTO). Through these experiments we ascertained C_t = 60, as the value providing the best results. Next, we applied the software to scale 2880 ionograms from the same campaign. These 2880 ionograms are out of the restricted data base used to fix C_t. The results obtained by the software have been compared to the ones given by an operator, and are reported in Tabs. 3. From these tables it is seen that more than 50% of the ionograms could not be manually scaled because of RF noise or the lack of data. A good agreement between manual and automatic scaling can be also seen, as more than the 80% of the analysed ionograms were correctly scaled by the software, according to the MUF values manually calculated by an expert operator. The false positive events created by the autoscaling algorithm are most probably due to the low quality of the ionograms.

This circumstance is confirmed by the data reported in Tabs. 4, which contains the results of the autoscaling program on a set of 384 high quality oblique ionograms, using a C_t = 60. In this case for all the ionograms of the data set an experienced operator has been able to calculate a MUF value, and the agreement between manual scaled and autoscaled MUF values is, greater than 96%. The

percentage of false positive events also drastically decreased to 3.9% as the quality of the ionograms increased.

4. Conclusions

A method for automatic scaling of oblique ionograms was introduced, based on the same technique as the Autoscala program. The method also provides a rejection procedure for ionograms that are considered to lack sufficient information, depicting a very good success rate, as reported in the Tabs. 1(d), 2(d), 3 and 4. From these tables it is also seen that the number of false positive events decrease for higher C_t. Observing the K_p index of each autoscaled ionogram, as reported in Fig. 2, we found that the behaviour of the autoscaling program does not depend on geomagnetic conditions.

The comparison between the values of the MUF provided by our software and those obtained from the same ionograms by an experienced operator indicate that the procedure developed for detecting the nose of oblique ionogram traces is sufficiently efficient and becomes much more efficient as the quality of the ionograms improves (Tabs. 4). These results demonstrate our program allows the real-time evaluation of MUF values associated with a particular radio link through an oblique radio sounding. The automatic recognition of the nose of the trace also allows us to determine the time taken by the radio wave to travel between the transmitter and receiver at frequencies at and just below the MUF.

References

Cesaroni, C., Scotto, C., Ippolito, A., 2013. An automatic quality factor for Autoscala foF2 values. Adv. Space Res., 51 (12), 2316-2321, doi: 10.1016/j.asr.2013.02.009.

Galkin, I. A., Khmyrov, G. M., Kozlov, A. V., Reinisch, B. W., Huang, X., Paznukhov, V. V., 2008. The ARTIST 5. In: Radio Sounding and Plasma Physics, AIP Conf. Proc., 974, 150–159, doi:10.1063/1.2885024.

Galkin, I. A., Reinisch, B. W., Huang, X., Bilitza, D., 2012. Assimilation of GIRO data into a real-time IRI. Radio Sci., 47 (4), RS0L07 [10 pages], doi:10.1029/2011RS004952.

Gilbert, J. D., Smith, R. W., 1988. A comparison between the automatic ionogram scaling system ARTIST and the standard manual method. Radio Sci., 23 (6), 968–974, doi: 10.1029/RS023i006p00968.

Huang, X., Reinisch, B. W., Kuklinski, W. S., 1996. Mid-point electron density profiles from oblique ionograms. Ann. Geophys. - Italy, 49 (4), 757-761, doi: 10.4401/ag-4012.

Norman, R. J., and Cannon, P. S., 1999. An evaluation of a new two-dimensional analytic ionospheric ray-tracing technique: Segmented method for analytic ray tracing (SMART). Radio Sci., 34 (2), 489-499, doi: 10.1029/98RS01788.

Pezzopane, M., Scotto, C., 2007. Automatic scaling of critical frequency foF2 and MUF (3000) F2: A comparison between Autoscala and ARTIST 4.5 on Rome data. Radio Sci., 42 (4), RS4003 [17 pages], doi:10.1029/2006RS003581.

Piggott, W. R., Rawer, K., 1972. U.R.S.I. Handbook of Ionogram Interpretation and Reduction. U.S. Department of Commerce National Oceanic and Atmospheric Administration-Environmental Data Service, Asheville, North Carolina, USA.

Reinisch, B. W., Huang, X., 1983. Automatic calculation of electron density profiles from digital ionograms: 3. Processing of bottomside ionograms. Radio Sci., 18 (3), 477–492, doi: 10.1029/RS018i003p00477.

Scotto, C., 2009. Electron density profile calculation technique for Autoscala ionogram analysis. Adv. Space Res., 44 (6), 756-766, doi: 10.1016/j.asr.2009.04.037.

Scotto, C., Pezzopane, M., 2002. A software for automatic scaling of f_oF2 and MUF(3000)F2 from ionograms. URSI XXVII General Assembly (http://www.ursi.org/Proceedings/ProcGA02/papers/p1018.pdf).

Scotto, C., Pezzopane, M., 2004. Software for the automatic scaling of critical frequency f_0F2 and MUF(3000) F2 from ionograms applied at the Ionospheric Observatory of Gibilmanna. Ann. Geophys. - Italy, 47 (6), 1783–1790, doi: 10.4401/ag-3375.

Stankov, S. M., Jodogne, J. C., Kutiev, I., Stegen, K., Warnan R., 2012. Evaluation of automatic ionogram scaling for use in real-time ionospheric density profile specification: Dourbes DGS-256/ARTIST-4 performance. Ann. Geophys. - Italy, 55 (2), 283-291, doi: 10.4401/ag-4976.

Table captions

Table 1. The behaviour of the algorithm to reject ionograms with insufficient information for different C_t on the oblique ionograms recorded on the Rome-Chania radio-link.

Table 2. Accurate and acceptable values for the test carried out with C_t = 150 on the oblique ionograms recorded on the Rome-Chania radio-link.

Table 3. (a) The behaviour of the algorithm to reject ionograms with insufficient information using C_t = 60 on the oblique ionograms recorded on the Kalkarindji-Culgoora radio-link. **(b)** Accurate and acceptable values for the test carried out with C_t = 60 on the oblique ionograms recorded on the Kalkarindji-Culgoora radio-link.

Table 4. (a) The behaviour of the algorithm to reject ionograms with insufficient information using C_t = 60 on the data set of 384 high quality oblique ionograms recorded on the Australian CUR-MTE radio-link. **(b)** Accurate and acceptable values for the test carried out with C_t = 60 on the data set of 384 high quality oblique ionograms recorded on the Australian CUR-MTE radio-link.

Figure captions

Figure 1. Autoscaled ionogram example: an ionogram for which both the operator and the software were able to provide the MUF value. The blue and red traces are the two analytic curves with C_{max}, the ones that best fit the oblique ionogram traces.

Figure 2. Time scale plot of the difference between the autoscaled MUFs and the manual scaled ones for three different C_t. The colours represent the different values of K_p index associated to each autoscaled ionogram. The number of autoscaled ionograms only depend on C_t and does not depend on K_p .

Figure 3. False positive example: an ionogram for which the operator was unable to provide the MUF value but not discarded by the software.

Table 1

(a)

C_t = 150	Scaled by the software		Discarded by the software	
	No. of cases	[%]	No. of cases	[%]
The operator did not scale the MUF	90	52.6	83	82.1
The operator scaled the MUF	81	47.4	18	17.9
Total	171		101	

(b)

C_t = 175	Scaled by the software		Discarded by the software	
	No. of cases	[%]	No. of cases	[%]
The operator did not scale the MUF	45	40.2	128	80.0
The operator scaled the MUF	67	59.8	32	20.0
Total	112		160	

(c)

C_t = 200	Scaled by the software		Discarded by the software	
	No. of cases	[%]	No. of cases	[%]
The operator did not scale the MUF	14	20.3	159	78.3
The operator scaled the MUF	55	79.7	44	21.7
Total	69		203	

(d)

C_t = 225	Scaled by the software		Discarded by the software	
	No. of cases	[%]	No. of cases	[%]
The operator did not scale the MUF	4	10.3	169	72.5
The operator scaled the MUF	35	89.7	64	27.5
Total	39		233	

(e)

C_t = 250	Scaled by the software		Discarded by the software	
	No. of cases	[%]	No. of cases	[%]
The operator did not scale the MUF	3	16.7	170	66.9
The operator scaled the MUF	15	83.3	84	33.1
Total	18		254	

Table 2

(a)

C_t = 150	Scaled by the software and by the operator	
	No. of cases	[%]
Accurate	30	37.04
Acceptable	79	97.53
Total	81	

(b)

C_t = 175	Scaled by the software and by the operator	
	No. of cases	[%]
Accurate	25	37.31
Acceptable	67	100.0
Total	67	

(c)

C_t = 200	Scaled by the software and by the operator	
	No. of cases	[%]
Accurate	21	38.18
Acceptable	55	100.0
Total	55	

(d)

C_t = 225	Scaled by the software and by the operator	
	No. of cases	[%]
Accurate	12	34.29
Acceptable	35	100.0
Total	35	

(e)

C_t = 250	Scaled by the software and by the operator	
	No. of cases	[%]
Accurate	4	26.67
Acceptable	15	100.0
Total	15	

Table 3

(a)

C_t = 60	Scaled by the software		Discarded by the software	
	No. of cases	[%]	No. of cases	[%]
The operator did not scale the MUF	109	15.2	1764	81.6
The operator scaled the MUF	610	84.8	397	18.4
Total	719		2161	

(b)

C_t = 60	Scaled by the software and by the operator	
	No. of cases	[%]
Accurate	565	92.7
Acceptable	610	100.0
Total	610	

Table 4

(a)

C_t = 60	Scaled by the software		Discarded by the software	
	No. of cases	[%]	No. of cases	[%]
The operator did not scale the MUF	0	0	0	0
The operator scaled the MUF	384	100.0	0	0
Total	384		0	

(b)

C_t = 60	Scaled by the software and by the operator	
	No. of cases	[%]
Accurate	345	89.9
Acceptable	369	96.1
Total	384	

Figure 1

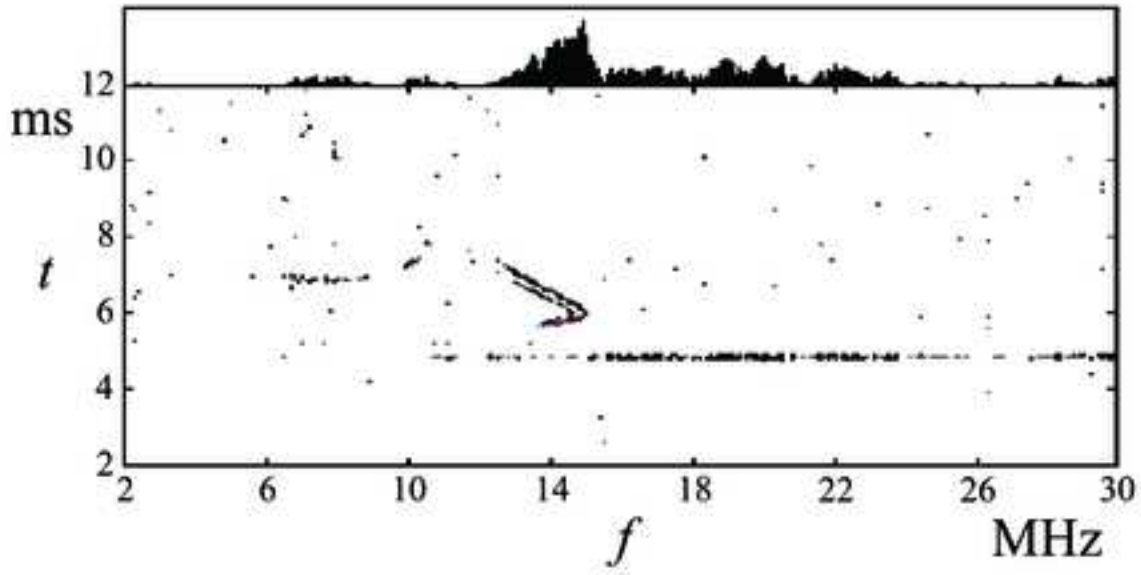

Figure 2

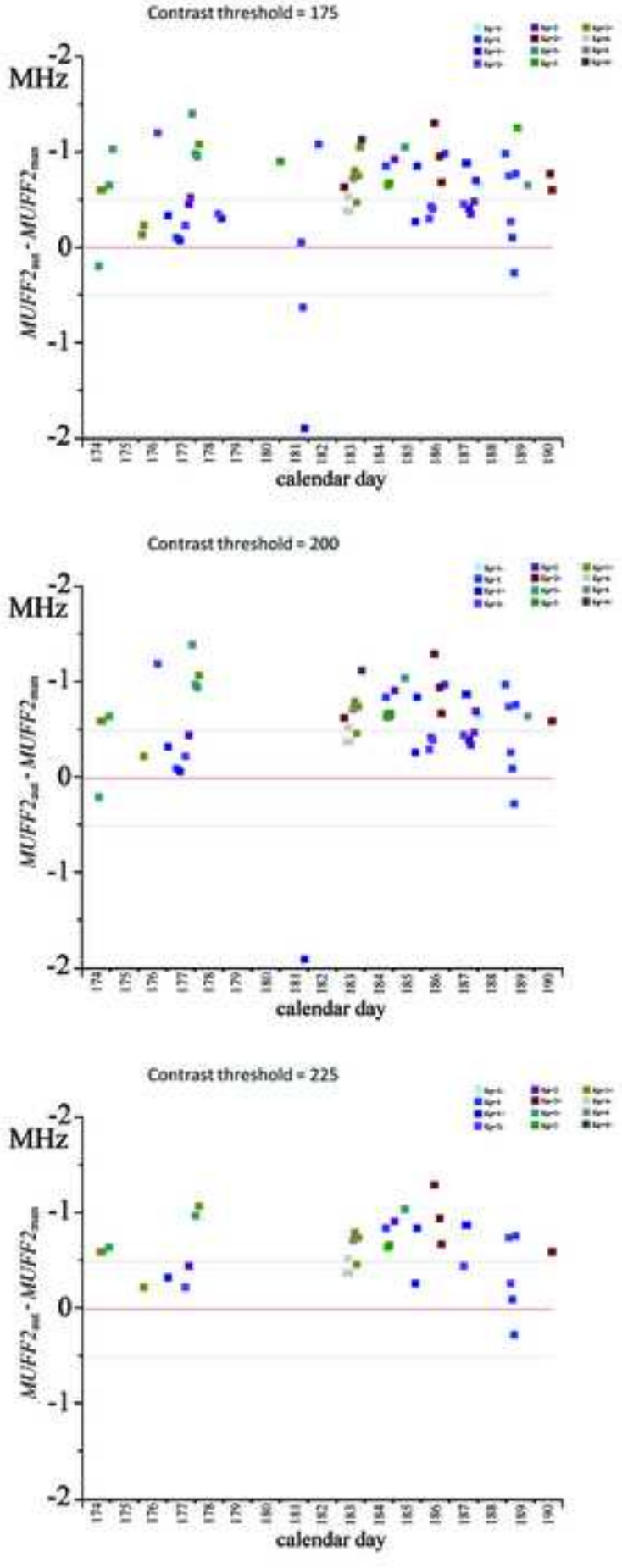
Contrast threshold = 175
MHz
$MUFF2_{ant} - MUFF2_{mean}$
calendar day
Contrast threshold = 200
MHz
$MUFF2_{ant} - MUFF2_{mean}$
calendar day
Contrast threshold = 225
MHz
$MUFF2_{ant} - MUFF2_{mean}$
calendar day

Figure 3